Pergamon

Biochemical Pharmacology, Vol. 50, No. 12, pp. 2057–2068, 1995.

0006-2952/95 $9.50 + 0.00

0006-2952(95)02108-6

INTERACTION BETWEEN THE Ah RECEPTOR AND PROTEINS BINDING TO THE AP-1-LIKE ELECTROPHILE RESPONSE ELEMENT (EpRE) DURING MURINE PHASE II [*Ah*] BATTERY GENE EXPRESSION

VASILIS VASILIOU, ALVARO PUGA, CHING-YI CHANG, M. WILSON TABOR and DANIEL W. NEBERT*

Department of Environmental Health, University of Cincinnati Medical Center, Cincinnati, OH 45267–0056, U.S.A.

(*Received* 14 *June* 1995; *accepted* 5 *September* 1995)

Abstract—We have studied three Phase II genes in the mouse dioxin-inducible [*Ah*] battery: *Nmo1* [encoding NAD(P)H:menadione oxidoreductase], *Ahd4* (encoding the cytosolic aldehyde dehydrogenase ALDH3c), and *Ugt1*06* (a UDP glucuronosyltransferase). Oxidant-induced *Nmo1* gene expression in the c^{14CoS}/c^{14CoS} mouse appears likely to be caused by homozygous loss of the fumarylacetoacetate hydrolase (*Fah*) gene on Chr 7 and absence of the enzyme (FAH), which leads to increased levels of endogenous tyrosine oxidative metabolites. We show here that increases in [*Ah*] Phase II gene expression in the *14CoS/14CoS* mouse are correlated with an AP-1-like DNA motif called the electrophile response element (EpRE), which has been found in the 5′ flanking regulatory regions of all murine [*Ah*] Phase II genes. Aromatic hydrocarbon response element (AhREs) are responsible for dioxin-mediated upregulation of all six [*Ah*] battery genes, and one or more AhREs have been found in the 5′ flanking regulatory regions of all of these [*Ah*] genes. Gel mobility shift assays, with a synthetic oligonucleotide probe corresponding to the EpRE, show that EpRE-binding proteins are more than twice as abundant in *14CoS/14CoS* than in the wild-type *ch/ch* nuclear extracts. Competition studies of EpRE-specific binding with an excess of EpRE, mutated EpRE, AP-1, AhRE3, mutated AhRE3, and C/EBPα oligonucleotides suggest that several common transcriptional factors bind to the EpRE and AhRE3 motifs. Two monospecific antibodies to the Ah receptor (AHR) protein block formation of an EpRE-specific complex on gel mobility electrophoresis. These data suggest that AHR (or AHR-related protein) might be an integral part of the EpRE-binding transcriptional complex associated with the oxidative stress response. To our knowledge, this is among the first reports of the same transcription factor operating at two different response elements upstream of a single gene.

Key words: [*Ah*] gene battery; Ah receptor; oxidative stress; hereditary tyrosinemia; binding of transcription factors; NAD(P)H:menadione oxidoreductase; aldehyde dehydrogenase; UDP glucuronosyltransferase

* Corresponding author. Tel. 513-558-0115; FAX 513-558-0925.

† Abbreviations: *c*, the murine albino locus encoding tyrosinase; Chr, chromosome; FAH, fumarylacetoacetate hydrolase encoded by the *Fah* gene; c^{14CoS}, allele in which there is a 3,800-kb deletion on mouse chromosome 7, including the *c* locus and the *Fah* gene; c^{ch}, wild-type allele; TCDD, 2,3,-7,8-tetrachlorodibenzo-*p*-dioxin or dioxin; AHR, Ah receptor; *p*HPP, *p*-hydroxyphenylpyruvic acid; HGA, homogentisic acid; *t*BHQ, *tert*-butylhydroquinone; NMO1, the TCDD-inducible NAD(P)H:menadione oxidoreductase (DT diaphorase, azo dye reductase) encoded by the murine *Nmo1* gene; ALDH3c, the TCDD-inducible cytosolic aldehyde dehydrogenase encoded by the murine *Ahd4* gene; UGT1*06, the TCDD-inducible UDP glucuronosyltransferase encoded by the murine *Ugt1*06* gene; GSTA1, the TCDD-inducible glutathione transferase Ya encoded by the murine *Gsta1* gene; EpRE, electrophile response element (also termed antioxidant response element, ARE); AhRE, aromatic hydrocarbon response element (also termed xenobiotic response element, XRE, and dioxin response element, DRE). By convention, murine genes include lower-case letters and italics, and other mammalian genes include all capital letters italicized, whereas the mRNA or enzyme (gene product) of all mammals including mouse are all capital letters and not in italics.

Mice having homozygous deletions near the *c*† locus on Chr 7 have been found to die *in utero* or shortly after birth, apparently as the result of hypoglycemia [1]. Subsequent studies of more than 3 dozen inbred mouse strains with overlapping radiation-induced chromosomal deletions around the albino (*c*) locus have suggested that one or more regulatory genes involved in different stages of development are located within this Chr 7 region (reviewed in [2–7]). Although some studies have focused on mutations that cause death at preimplantation stages of development [6], work in our laboratory has centered on the c^{14CoS} mutation—which has the smallest deleted region of all mutant lines studied [2, 3, 7].

Loss of both copies of a dominant positive regulatory gene would lead to decreases in expression of those genes under its control. For example, in contrast to the c^{ch}/c^{ch} wild-type and the c^{ch}/c^{14CoS} heterozygote, the c^{14CoS}/c^{14CoS} mouse—homozygous for a 3800-kb deletion on Chr 7 around the *c* locus—fails to activate a battery of genes involved in neonatal liver functions and dies during the first day postpartum [2, 3, 7].

One locus, believed to be necessary for survival beyond birth and proposed to play an important role in

perinatal differentiation of the hepatocyte [2], has been variously designated *hsdr1* (hepatocyte-specific developmental regulator-1) [2, 5] and *alf* (albino lethal factor) [8]. This phenotype fails to activate several hepatic enzymes involved in gluconeogenesis. For example, there are decreases in glucose-6-phosphatase, tyrosine aminotransferase, phosphoenolpyruvate carboxykinase, glucokinase, and CYP2E1 [1, 9–12], presumably due to loss of the *alf* gene, which might encode a putative positive *trans*-acting factor. However, *14CoS/14CoS* mice also show decreases in albumin, α-fetoprotein, transferrin, and metallothionein [4, 13], altered expression of genes encoding the urea-cycle enzymes [14], and changes in tubule cell development in the fetal kidney [8]. In addition, mRNA levels for three transcription factors—C/EBPα, HNF-1α and HNF-4—are all strikingly decreased in the *14CoS/14CoS* deletion homozygotes [5, 8, 12, 15]. It should be emphasized that, on average, approximately 30 genes would be expected to occupy a 3800-kb region of genomic DNA [16, 17]. In summary, these data suggest that multiple signal transduction pathways and numerous genes might be affected as the result of this 3800-kb deletion on mouse Chr 7.

In contrast to the loss of positive regulation described above, there is evidence for increases in the activity of some genes [7]. Expression of three growth arrest- and DNA damage-inducible (*gadd*) genes [18], plus four genes in the murine aromatic hydrocarbon-responsive [*Ah*] battery [7, 19–25] is markedly increased, rather than decreased, in the *14CoS/14CoS* homozygote. The murine [*Ah*] gene battery comprises at least six dioxin-inducible genes: two Phase I cytochrome P450 genes, *Cyp1a1* and *Cyp1a2*, and four Phase II genes: *Nmo1*, *Ahd4*, *Ugt1*06*, and *Gsta1* (reviewed in [23, 24]). All six genes are inducible by environmental chemicals that are AHR ligands such as TCDD. The induction process requires a functional AHR, acting through a transcriptional complex binding to the DNA motif called the AhRE. The chromosome 7-mediated pathway appears to affect principally the [*Ah*] Phase II genes [7, 24].

Recent studies implicate the loss of a murine Chr 7 gene as the cause of an oxidative stress response. Besides the four [*Ah*] Phase II genes (which are believed to be protective against oxidative stress [7]), superoxide dismutase, glutathione reductase, glutathione peroxidase, and glucose-6-phosphate dehydrogenase activities—enzymes not in the dioxin-inducible [*Ah*] battery but important in the redox cycling of oxidants—are also elevated in newborn liver of the untreated *14CoS/14CoS* mouse [25]. Interestingly, newborn liver or SV40-transformed hepatocyte cultures from the *14CoS/14CoS* mouse exhibit elevated NADPH and GSH levels, prostaglandin A_2 induction, and enhanced arachidonic acid release, as compared with that from the *ch/ch* or *ch/14CoS* mouse [25–27]. Several other enzymes and proteins not associated with oxidative stress were shown to be the same in *14CoS/14CoS* and *ch/ch* mice [2, 25].

The fumarylacetoacetate hydrolase (*Fah*) gene is located in the region on Chr 7 that is deleted in *14CoS/14CoS* mice [28, 29]. Two laboratories studied *14CoS/14CoS* mice that received the *Fah* transgene [30] and C57BL/6 wild-type mice that have a homozygous disruption in the *Fah* gene [31]. They have shown that, not only can the lethal phenotype of *14CoS/14CoS* newborns be corrected by insertion of the *Fah* gene, but also the *Nmo1* and *gadd* induction appears to be caused by absence of the *Fah* gene and *Fah* gene insertion into *14CoS/14CoS* mice restores the *Nmo1* and *gadd* gene expression to basal wild-type levels.

The upstream regulatory regions of all four murine [*Ah*] Phase II genes (but not *Cyp1a1* or *Cyp1a2*) contain at least one EpRE [22]; (reviewed in [24]). The EpRE has an AP-1-like DNA motif [32, 33] that responds to oxidative stress, (i.e. endogenous or exogenous lipid peroxidation, quinones, and other electrophilic metabolites) [34]. In the absence of FAH or in the presence of excessive amounts of endogenous or exogenous oxidative metabolites, therefore, the cell appears to undergo an oxidative stress response, inducing the [*Ah*] Phase II genes as well as other genes in the appropriate signal transduction pathways—including *c-fos* [29]—to combat the oxidative stress. In the present report, we have used gel mobility shift and antibody supershift assays to examine for the presence or absence of specific EpRE-binding proteins in *14CoS/14CoS* and *ch/ch* cell lines. We also demonstrate an interrelationship between DNA-binding proteins that interact with both the AhRE and the EpRE DNA motifs.

MATERIALS AND METHODS

Mouse colony

In 1986, male and female *ch/14CoS* mice were generous gifts of Liane B. Russell (Oak Ridge, TN), and breeding has been carried out in the mouse colony of this laboratory since that time. The three genotypes can easily be identified from their phenotypes in utero or after birth: the *14CoS/14CoS* has no eye pigmentation and dies during the first 24 hr postpartum, the wild-type *ch/ch* has dark eye pigmentation and chinchilla coat color, and the *ch/14CoS* is completely viable and has intermediate eye pigmentation and dilute brown coat color [2, 7].

Cell culture conditions

The mouse hepatoma Hepa-1 wild-type (*wt*) cell culture [35] has been characterized in this laboratory for more than two decades [36]; the Hepa-1 *wt* clone, Hepa-1c1c7, and its CYP1A1 metabolism-deficient *c37* mutant [37] were generous gifts of Noll Hankinson (UCLA, Los Angeles, CA). The *wt* cell line was routinely grown in modified Eagle's α-medium containing 5% fetal calf serum.

Development and characterization of the *ch/ch*, *ch/14CoS*, and *14CoS/14CoS* simian virus (SV40)-transformed cell lines have been detailed previously [27]. With regard to elevated *Nmo1*, *Ahd4*, and *Ugt1*06* gene expression in the *14CoS/14CoS* but not in the *ch/14CoS* or *ch/ch* cell lines, these phenotypic differences have remained stable for more than 8 years. The *14CoS/14CoS*, *ch/14CoS*, and *ch/ch* cell lines are routinely grown at 34°C in 75-cm^2 flasks containing 15 mL of Dulbecco's Modified Eagle's Medium (DMEM) supplemented with 5% fetal bovine serum, 0.1% gentamycin, and 26 mM $NaHCO_3$, under 95% air:5% CO_2. Cells in exponential growth (about 70% confluent) were used for these studies. When needed, cells were treated with TCDD (10 nM) or *tert*-butylhydroquinone (tBHQ) (25 or 50 μM) for 6 or 12 hr; controls received the vehicle *p*-dioxane or dimethylsulfoxide (0.25%) alone.

RNA extraction and Northern blots

RNA was extracted by the acid guanidinium thiocyanate method [38]. Total RNA (20 μg) was separated in formaldehyde-agarose gels and transferred to Nytran membranes. Prehybridizations and hybridizations were carried out at 42°C in a solution containing 50% deionized formamide, 6 × SSC, 2.5 × Denhardt's solution, 0.5% sodium dodecylsulfate (SDS), and denatured salmon sperm DNA (0.1 mg/mL). After hybridization for 16–20 hr, the filters were washed twice in 2 × SSC and 0.1% SDS for 10 min at room temperature and then twice in 0.1 × SSC and 0.1% SDS for 30 min at 45°C. The filters were then exposed for 24–48 hr to Kodak XAR-5 film at −70°C with intensifying screens. Probes included the mouse NMO1 [22], ALDH3c [20, 21], and UGT1*06 [39] full-length cDNAs.

Determination of p-*hydroxyphenylpyruvic acid (*p*HPP) and homogentisic acid (HGA) concentrations in newborn liver and in cell cultures*

*p*HPP, HGA, and *tert*-butylhydroquinone (tBHQ) were obtained from Sigma. Both were stored at 0°C in a desiccator until stock solutions were made for use as standards. *o*-Phosphoric acid (99% purity) was obtained from Fluka Chemical, Buchs, Switzerland. ASTM Type I water [40] was used for making aqueous solutions of these reagents. Optima-grade$^{(R)}$ solvents for high performance liquid chromatography (hplc) were obtained from Fisher Scientific. All other chemicals were of reagent grade or better and obtained from Fisher Scientific.

Both hepatic homogenates and cell suspensions were examined for *p*HPP and HGA concentrations. Newborn *14CoS/14CoS* and *ch/ch* liver samples (100-mg aliquots) were homogenized in 10 volumes (10% w/v) of 20 mM Tris buffer (pH 7.5) containing 1 mM dithiothreitol and 20% (v/v) glycerol. A 500-μL aliquot of homogenate was combined with 50 μL 5.8 M perchloric acid, and the samples were vortexed vigorously for 30 sec. The *14CoS/14CoS* and *ch/ch* cell cultures were treated with trypsin and resuspended in growth medium. For each 100-μL aliquot of cells, 10 μL 5.8 M perchloric acid was added, and the samples were vortexed as above. The newborn liver and cell culture samples were then centrifuged at 1000 × g for 10 min, following which the aqueous supernatant fluid was removed and the volume recorded. If sample analysis could not be performed immediately, supernatant fluids were stored at −4°C until time of analysis. For analysis, a 200- to 300-μL aliquot of the supernatant fluid was pipetted into a 4.0-mL amber WISPR vial (Sun Brokers Inc., Wilmington, NC) which had been fitted with a LO-volume^{R} insert.

Sample analysis was performed *via* a modification of the method of Bory *et al.* [41] using principles described by Tabor [42]. Standards plus the samples were analyzed using a Waters Associates hplc system consisting of the following configuration: model M712 WISPR autoinjector, two model M590 pumps, a model M680 gradient controller, and a M990+ photodiode array detector with a NEC APC IV Powermate 2 data system. Chromatographic separation of the analytes was accomplished utilizing a μBondapak^{R} C_{18} radial compression module column (8 mm × 10 cm) with an isocratic mobile phase of 70% aqueous 12 mM *o*-phosphoric acid:30% methanol (v/v), at a flow rate of 1.00 mL/min. Eluate detection was carried out by continuous scanning from 200 to 400 nm with an average sampling time of 70 msec per scan. *p*HPP and HGA were quantitated at 302 and 293 nm, respectively, using standard curves generated from authentic standards dissolved in the hplc mobile phase, which represented concentrations from 1 nM to 10 μM. Solutions of standards were stored at 2°C in foil-wrapped amber WISPR vials and were determined to be stable (i.e., with changes in concentrations of <3% over a 10-day period).

Determination of p*HPP, HGA, and tBHQ toxicity in cell cultures*

The *wt* mouse hepatoma cell line Hepa-1c1c7 and the SV40-transformed *14CoS/14CoS* and *ch/ch* cell lines were treated for 6–24 hr with *p*HPP, HGA, or tBHQ (ranging from 1 nM to 5 mM). All three chemicals were first dissolved in DMSO; final DMSO concentrations were ≤0.25% which caused no toxic effects. The amount of toxicity was assessed by light microscopy, cell counts, and trypan blue dye exclusion.

Gel mobility shift/antibody supershift analysis

Nuclear extracts from untreated *14CoS/14CoS, ch/14CoS,* and *ch/ch* cells were prepared by procedures described elsewhere [43]. Double-stranded synthetic 41-mers containing the EpRE [32] and a mutant EpRE were prepared. The sense strand of the murine EpRE used in this study was: 5′TAGCTTGGAAATGACATTGCTAATGGTGACAAAGCAACTTT-3′, where the underlined bases are regarded as the consensus EpRE sequence [33]. The sense strand of the mutant EpRE (mEpRE) was also used: 5′-TAGCTTGGAAATGACATTGCTAATGTGTCACCCTAAACTTT-3′, where the underlined bases show deviation from the consensus EpRE sequence.

These oligos were end-labeled by T4 polynucleotide kinase and [γ-^{32}P]ATP for use in the gel mobility shift/antibody supershift assays. The binding reactions were carried out by incubating 10 μg of crude nuclear extract with 0.1 ng of the labeled probe (10,000 to 15,000 cpm) in a buffer containing 10 mM Hepes, 50 mM KCl, 1 mM EDTA, 1 mM dithiothreitol, 5 mM $MgCl_2$, 10% glycerol, and 50 mg/mL poly(dI-dC) for 20 min at room

Table 1. Oligonucleotides used in the present study

Gstal EpRE:	-754 TAGCTTGGAAA**TGACATTGC**TAATGG**TGACAAAGC**AACTTT-714
Gstal mEpRE:	-744 A**TGACATTGC**TAATG**TGTCACCCTA**AACTTT -714
AP-1:	CTAGTGA**TGAGTCA**GCCGGATC
Cyp1al AhRE3:	-977 TGCCCCGGA**GTTGCGTGAGAA**GAGGCCTGGA-1066
Cyp1al mAhR3:	TGCCCCGGA**TGGTATGTCT**CCGAGGCCTGGA
Oct-1:	GATCGAATGCAAATCACTAGCT

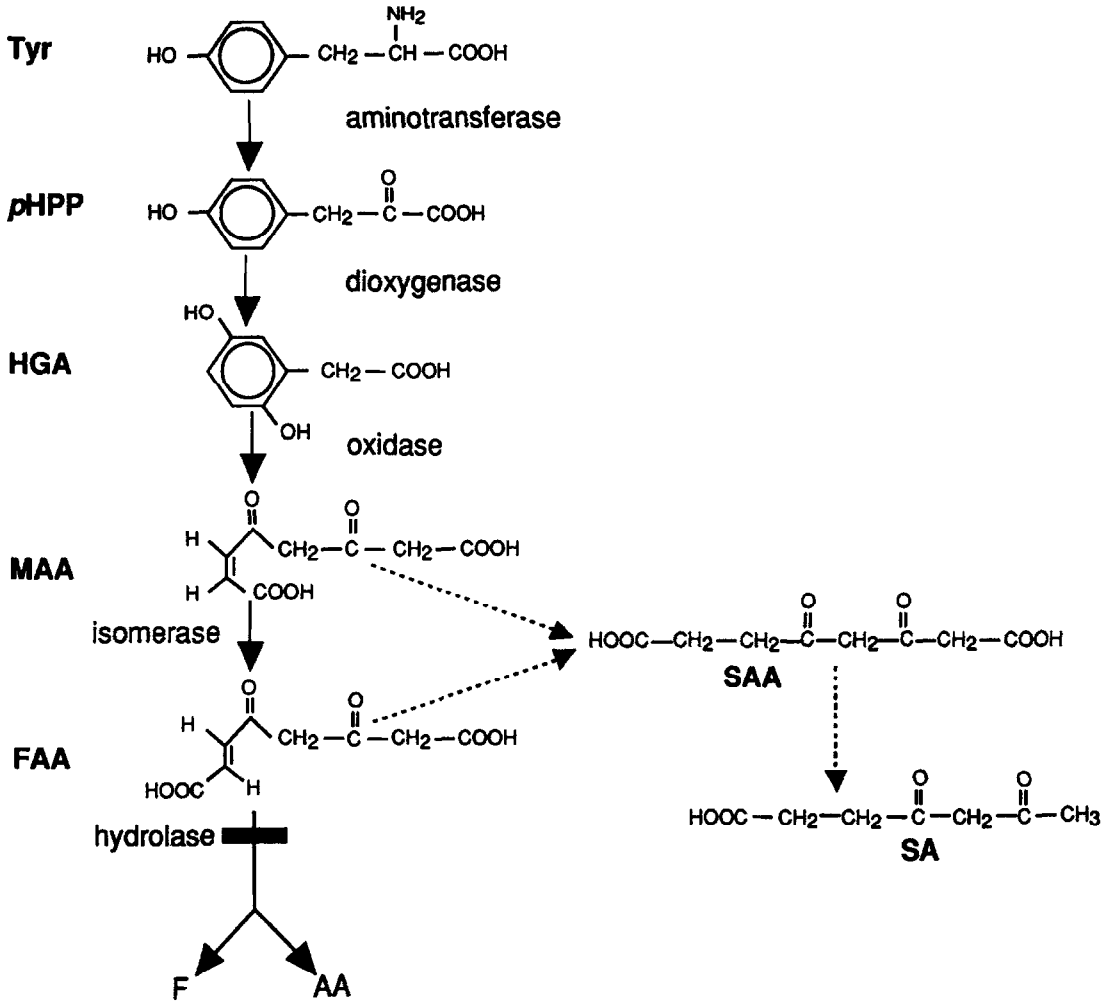

Fig. 1. Tyrosine degradation pathway. Tyr, tyrosine; *p*HPP, *p*-hydroxyphenylpyruvate; HGA, homogentisic acid; MAA, maleylacetoacetate; FAA, fumarylacetoacetate; F, fumarate; AA, acetoacetate; SAA, succinylacetoacetate; SA, succinylacetone. *Dashed lines* denote metabolic steps in which the exact enzymes and mechanisms involved are not known. FAA hydrolase, encoded by the *Fah* gene, has been shown to be absent in the *14CoS/14CoS* mouse [28, 29].

Table 2. *p*HPP and HGA metabolite concentrations in the *14CoS/14CoS* and *ch/ch* newborn liver and in the cell culture lines

Sample	Metabolite	Concentration* in homogenate (mM)	Concentration (pmoles/cell)
Newborn liver:			
14CoS/14CoS	*p*HPP	<0.10	<0.01
ch/ch		<0.10	<0.01
14CoS/14CoS	HGA	7.2 ± 1.2	0.80 ± 0.14
ch/ch		4.4 ± 0.9	0.65 ± 0.16
Cell culture lines:			
14CoS/14CoS	*p*HPP	<0.10	<0.01
ch/ch		<0.10	<0.01
14CoS/14CoS	HGA	4.1 ± 0.6	1.1 ± 0.13
ch/ch		3.1 ± 0.5	0.74 ± 0.11

Values are expressed as the means ±SD (N = duplicate determinations from three separate experiments).

* Protein concentrations of newborn liver homogenates or of pelleted cell homogenates, ranged between 2.5 and 6.0 mg per mL.

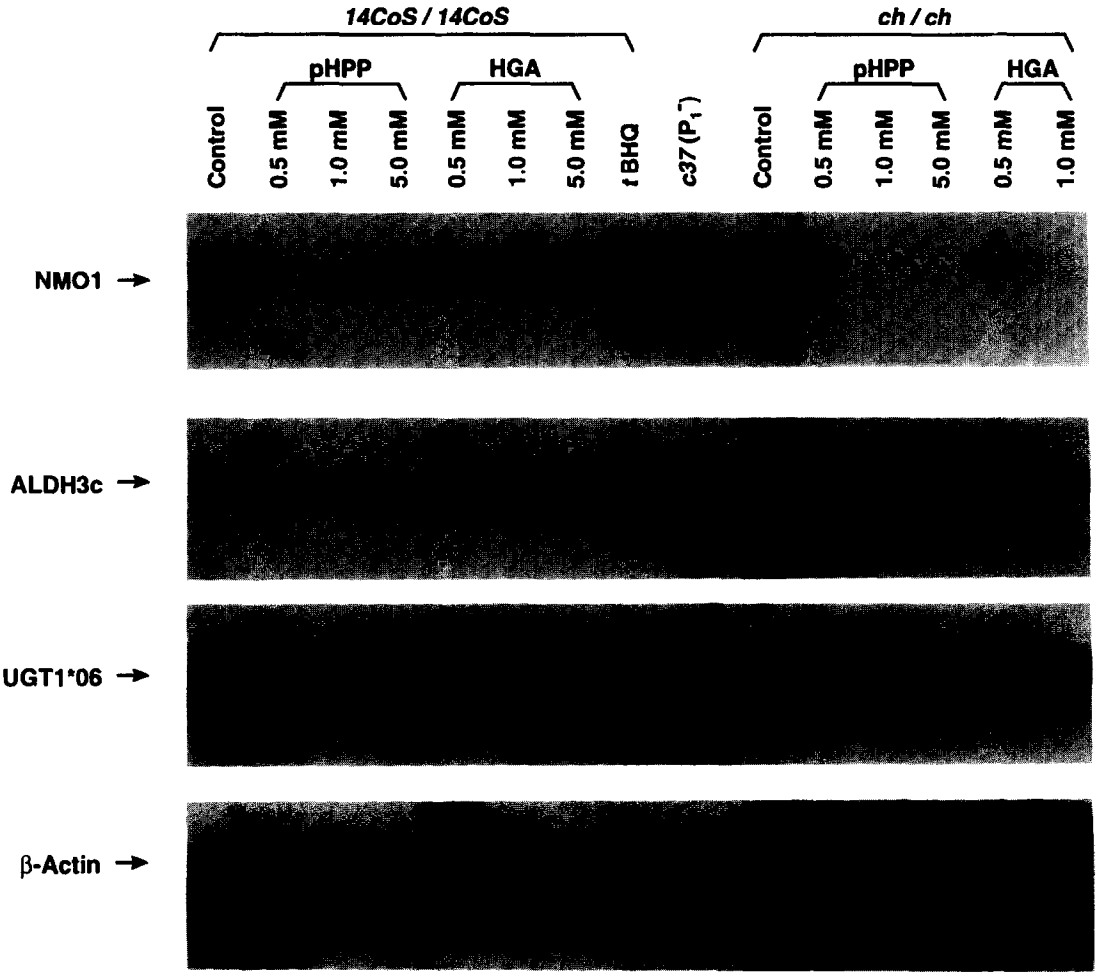

Fig. 2. Northern hybridization analysis. NMO1, ALDH3c, and UGT1*06 mRNA levels were determined in untreated *14CoS/14CoS* cells, in *14CoS/14CoS* and *ch/ch* cells after *p*HPP or HGA treatment, in *14CoS/14CoS* cells after 25 μM tBHQ treatment, and in the untreated CYP1A1 metabolism-deficient *c37* cells. Treatments were for 12 hr in the experiments shown. Levels of β-actin mRNA are included to standardize the amount of RNA loaded per lane.

temperature. In the competition experiments, a 200-fold molar excess of unlabeled (EpRE, or mutant mEpRE) DNA was preincubated with the reaction mixture for 10 min before the addition of the labeled probe. The binding reactions were separated by 6% polyacrylamide gel electrophoresis at 20 mA in 0.5X TBE (89 mM Tris, 89 mM boric acid, 2 mM EDTA, pH 8.3). The gel was then dried and exposed to XAR-5 film (Kodak).

Double-stranded synthetic oligonucleotides containing the AhRE3 and the mutant AhRE3, previously described [44], the AP-1 motif [33], and the C/EBPα recognition sequence [45] were used as nonlabeled competitors at several concentrations of fold excess. The oligonucleotides used in these studies are summarized in Table 1. Preimmune serum and immune rabbit antibodies to the murine AHR bHLH region (PI bHLH and αbHLH, respectively) and glutamine-rich region (PI QR and αQR, respectively) [46] were developed by immunization with bHLH (amino acids 1–347) or QR (amino acids 418–804) peptides that had been expressed in bacteria from recombinant cDNA clones. Immune IgG was purified by affinity chromatography on an antigen column, followed by a protein A-sepharose column, using standard purification techniques. An antibody to Ah receptor nuclear translocator (ARNT) was a generous gift of Gary Perdew (Purdue University). Preimmune serum or antibody (ranging from 1.5 to 6.0 μg) was added to the nuclear extracts and stirred for 15 min at room temperature prior to gel electrophoresis.

RESULTS AND DISCUSSION

Measurement of pHPP *and HGA concentrations in newborn liver and cell cultures*

We have previously shown that mRNA levels of the [*Ah*] Phase II genes are markedly elevated in the *14CoS/14CoS*, but not in the *ch/ch* or *ch/14CoS*, newborn liver or cell lines derived from these livers [7, 19–24]. Although one possibility is that these genes are putatively "depressed" due to deletion of a repressor [7, 24], another possibility is that these genes are induced by endogenous electrophilic metabolites. The fumarylacetoacetate hydrolase (*Fah*) gene, encoding an enzyme involved in tyrosine metabolism (Fig. 1), is present in the deleted region of Chr 7 and, therefore, missing in the *14CoS/14CoS* mouse [28, 29]. It now appears that FAH

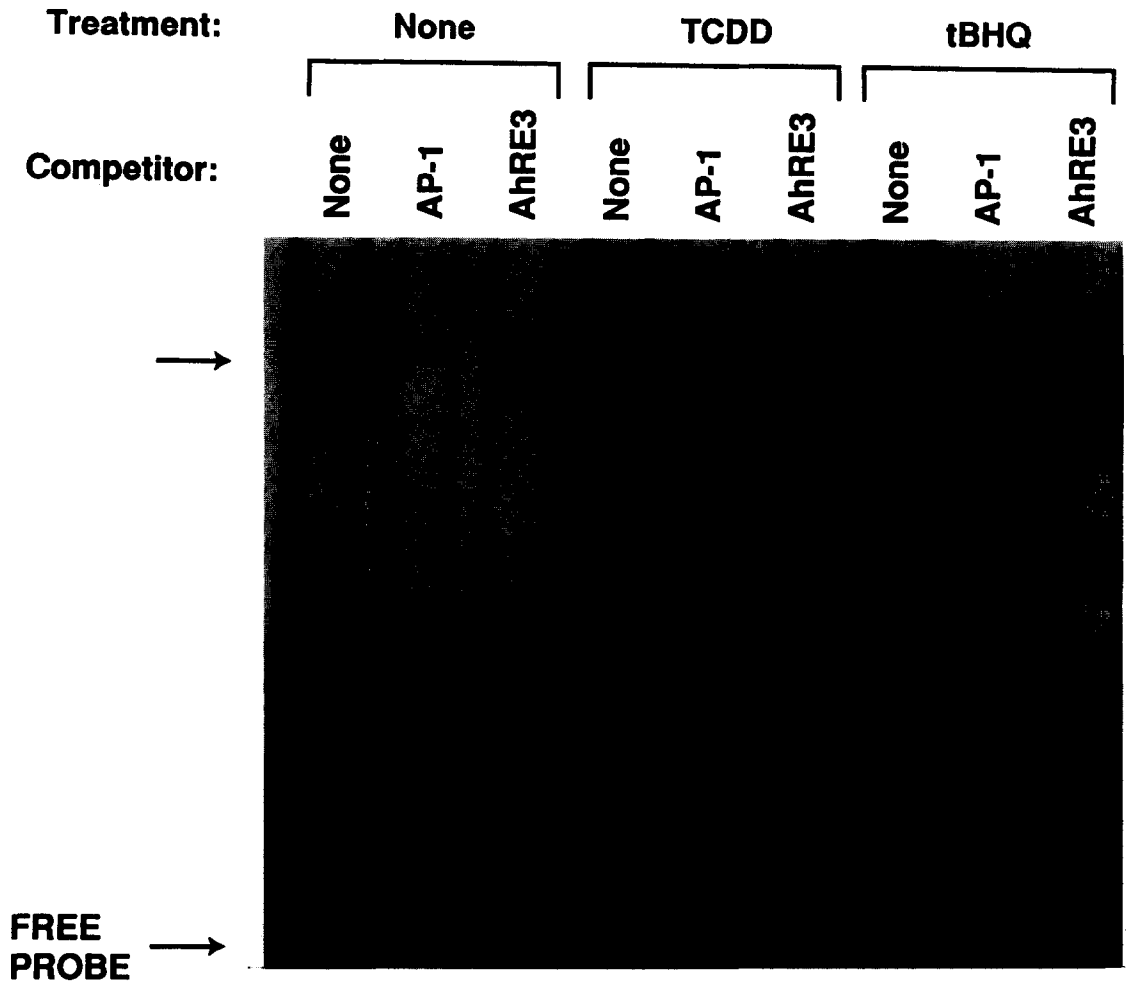

Fig. 3. Gel mobility shift analysis of Hepa-1 *wt* nuclear extracts probed with the radiolabeled *Gsta1* EpRE. Cells were treated with 10 nM TCDD, 50 μM tBHQ or vehicle alone for 6 hr. The EpRE-specific band (denoted by *arrow*) was competed with 150-fold excess of nonlabeled AP-1 or AhRE3 oligonucleotides.

deficiency might cause the accumulation of toxic tyrosine metabolites, which play a role in an oxidative stress response. We attempted to detect elevated levels of two metabolites in the tyrosine degradative pathway, *p*HPP and HGA.

Table 2 shows that no striking differences in *p*HPP or HGA levels were found, between *14CoS/14CoS* and *ch/ch* newborn liver samples or between the *14CoS/14CoS* and *ch/ch* established cell lines. Interestingly, *p*HPP was not detectable in either the intact liver or the cell cultures, suggesting that *p*HPP levels might be negligible due to relatively high levels of *p*HPP dioxygenase for which *p*HPP is the substrate (Fig. 1), or due to its high reactivity and, therefore, relatively short half-life. On the other hand, HGA was detectable at concentrations between 3.1 to 7.2 mM in the homogenates; this was calculated to range between 0.65 and 1.1 pmoles per cell. If HGA is also highly unstable and were to react covalently and rapidly with subcellular macromolecules, this might explain why no striking differences were found between the *14CoS/14CoS* and *ch/ch*.

Our negative results can likely be explained on the basis that these metabolites are highly reactive and have relatively short half-lives, as discussed in detail by Grompe and coworkers [31]. In humans, FAH deficiency causes hereditary tyrosinemia type I (HT1), a severe autosomal recessive inborn error of metabolism [47]. Succinylacetone (Fig. 1) is the hallmark metabolite of human tyrosinemia; yet, although usually detected in plasma and urine, succinylacetone is often not detected in human liver [48]. Succinylacetone was measured in *14CoS/14CoS* newborn liver and elevated levels were not detected [49]. If increases in this major metabolite from FAH deficiency cannot be detected, perhaps it is not surprising that we were unable to find (Table 2) significant differences in *p*HPP or HGA between *14CoS/14CoS* and *ch/ch* newborn liver, as well as between the two cell lines in culture.

Many of the defects and the symptomatology between human HT1 and the *14CoS/14CoS* mouse are similar, although there are some phenomena that differ (reviewed in [31]). Interestingly, there is evidence for depletion of intracellular reducing compounds, such as reduced glutathione (GSH), in red cells of HT1 patients [50]. In contrast, GSH levels are approximately 3 times higher in *14CoS/14CoS* than in *ch/ch* cells [27]. Further work is needed to understand the regulation of GSH levels in these cells.

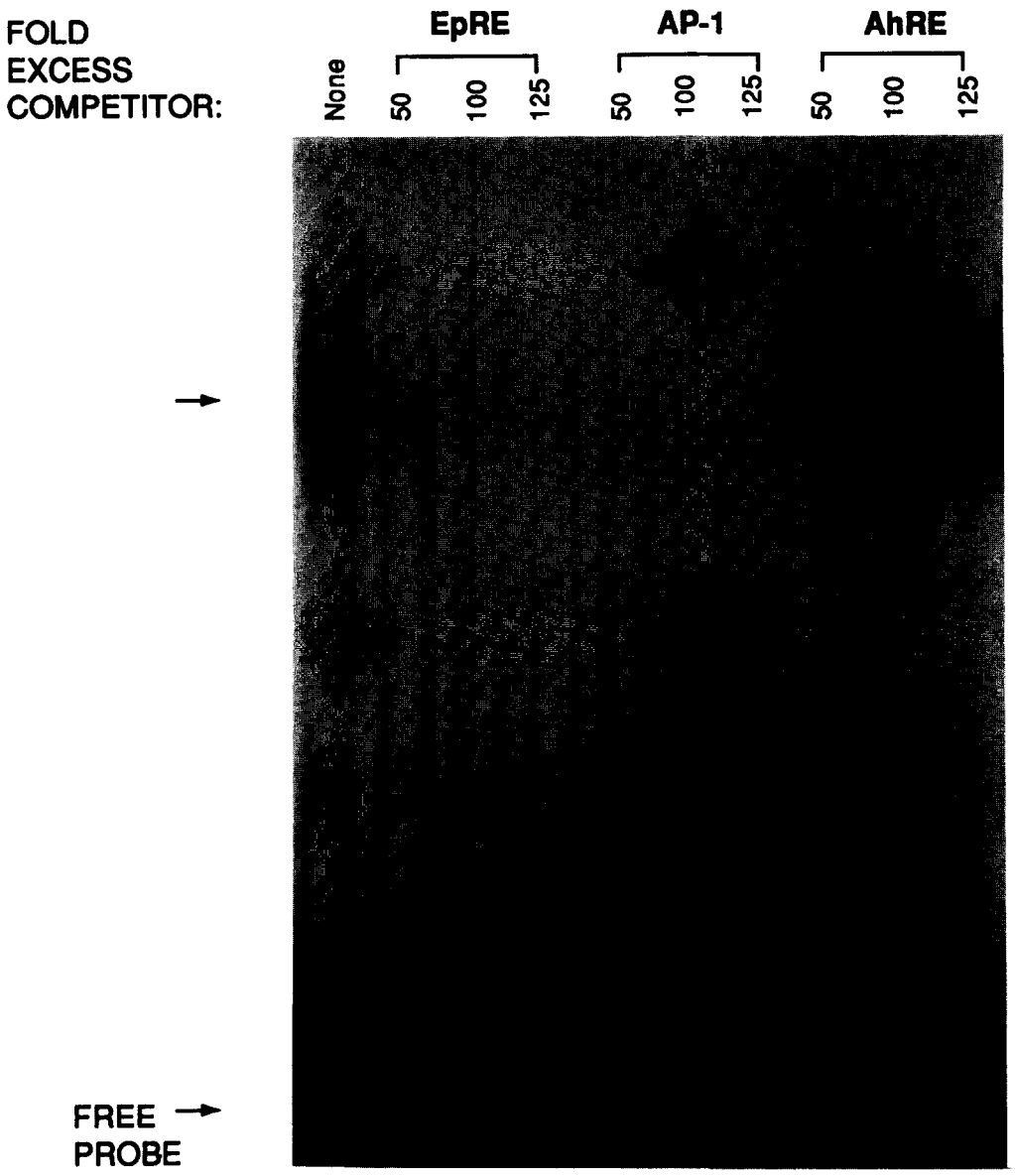

Fig. 4. Gel mobility shift analysis of untreated *ch/ch* nuclear extracts probed with the radiolabeled *Gsta1* EpRE in the presence of 50-, and 125-fold excess of nonlabeled EpRE, AP-1, or AhRE3 oligonucleotides. The EpRE-specific band is denoted by the *arrow*.

Toxicity in 14CoS/14CoS *and* ch/ch *cells after* p*HPP or HGA treatment*

We next determined whether addition of *p*HPP or HGA to the growth medium, up to concentrations causing toxicity and cell death, might induce NMO1, ADLH3c, and UGT1*06 mRNA levels. Treating *14CoS/14CoS* and *ch/ch* cells with *p*HPP or HGA concentrations between 1 nM and 5 mM, we observed no toxicity below 0.5 mM. We found that *p*HPP treatment for 12 hr—at concentrations of 0.5 mM, 1.0, and 5.0 mM—produced about 0%, 5%, and <10% cell death in *14CoS/14CoS* cells, respectively, and about 0%, 10%, and 30% in *ch/ch* cells, respectively. We determined that HGA for 12 hr—at concentrations of 0.5 mM, 1.0, and 5.0 mM—produced about 5%, 10%, and <30% cell death in *14CoS/14CoS* cells, respectively, and about 25%, 50%, and >95% in *ch/ch* cells, respectively. We also found that *t*BHQ for 12 hr—at 25 μM caused <5% cell death in *14CoS/14CoS* cells but >90% cell death in *ch/ch* cells (data not shown). We believe that these observations of increased protection in the *14CoS/14CoS* line are related to the 3-fold elevated GSH levels that have been found in *14CoS/14CoS* cells [27].

*NMO1, ALDH3c, and UGT1*06 mRNA levels in* 14CoS/14CoS *and* ch/ch *cells after* p*HPP or HGA treatment*

Would the addition of tyrosine oxidative metabolites cause the *ch/ch* wild-type cell line to behave like the FAH-deficient *14CoS/14CoS* line? Fig. 2 shows that, when near-toxic and toxic levels of *p*HPP and HGA had been added to the *14CoS/14CoS* and *ch/ch* cell lines, there were no concentrations of either tyrosine metabolite that induced NMO1 or ALDH3c mRNA in the wild-

Table 3. Densitometric analysis: Competition of EpRE-specific band with nonlabeled EpRE, AP-1 and AhRE3 oligonucleotides

Competitor	Fold excess	% EpRE-specific band
None		100%
EpRE	50:1	23
	100:1	10
	125:1	<1
AP-1	50:1	<1
	100:1	<1
	125:1	<1
AhRE3	50:1	90
	100:1	80
	125:1	50

Values are expressed as the EpRE-specific band divided by the Oct-1 band, as estimated from densitometric analysis of three separate experiments (i.e. nuclear extracts from three different cultures of each cell line).

type *ch/ch* line, to levels that approach those seen in the untreated *14CoS/14CoS* line. On the other hand, 1.0 mM *p*HPP and both 0.5 and 1.0 mM HGA appeared to increase UGT1*06 mRNA levels, which already have a high constitutive level in the *ch/ch* cells (but which are much higher in the untreated *14CoS/14CoS* line).

NMO1 and ALDH3c mRNA levels appeared to be slightly diminished in *p*HPP- and HGA-treated *14CoS/14CoS* cells, as compared with that in untreated *14CoS/14CoS* cells; we do not know the reason for this observation nor can we offer reasonable speculation. An exception was the dose of 5.0 mM HGA given to *14CoS/14CoS* cells, in which some increase in ALDH3c mRNA was consistently seen.

The CYP1A1 metabolism-deficient *c37* mutant exhibits higher NMO1, ALDH3c, and UGT1*06 mRNA levels, compared with that of the untreated *14CoS/14CoS* line; these mRNA levels in *c37* are very much higher than that of the untreated *ch/ch* line (Fig. 2). This laboratory has previously demonstrated these data for the NMO1, ALDH3c, and UGT1*06 mRNAs [20–22].

tBHQ is a potent electrophilic oxidant. tBHQ treatment of *wt* and *c37* cells has been shown to cause small increases in ALDH3c mRNA concentrations [51]. NMO1 mRNA was strikingly increased by tBHQ in *14CoS/14CoS* cells (Fig. 2) and in *ch/ch* cells (data not shown), whereas tBHQ had little or no effect on ALDH3c and UGT1*06 mRNA induction. These findings underscore the fact that different [*Ah*] Phase II genes respond differentially to oxidative chemicals—perhaps due to variations in the levels of electrophiles, redox factors, and/or transcription factors in specific cell types or in subcellular compartments [31].

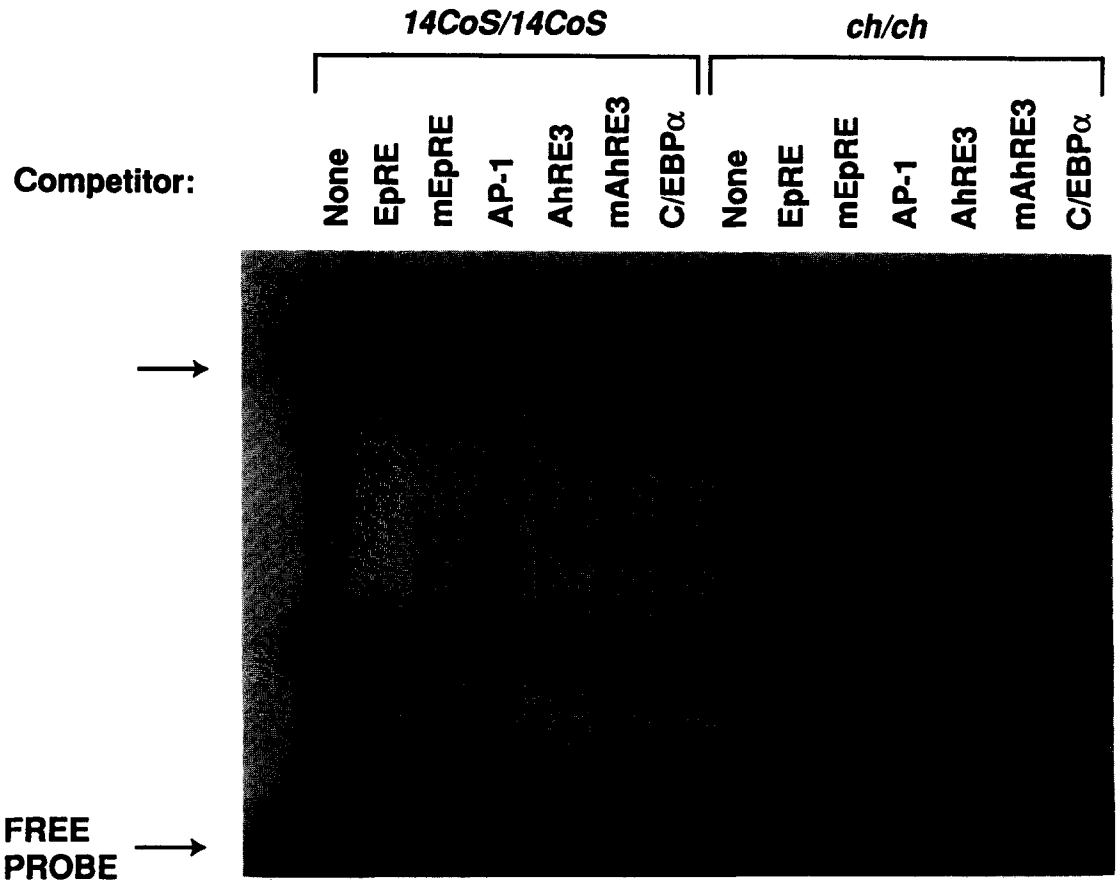

Fig. 5. Gel mobility shift analysis of untreated *14CoS/14CoS* and *ch/ch* nuclear extracts probed with the radiolabeled *Gsta1* EpRE in the presence of 150-fold excess of the following nonlabeled oligonucleotides: EpRE, mutated EpRE (mEpRE), AP-1, AhRE3, mutated AhRE3 (mAhRE3), and C/EBPα. The EpRE-specific band is denoted by the *arrow*.

Table 4. Relative intensity of the EpRE-specific band in untreated *ch/ch* and *14CoS/14CoS* cells

Cells	EpRE/Oct-1 Ratio*
ch/ch	0.32 ± 0.10
14CoS/14CoS	0.80 ± 0.18†

* Values are expressed as the means ± SD of the relative band intensity (EpRE band divided by the Oct-1 band), as estimated from densitometric analysis of 5 separate experiments (i.e. nuclear extracts from 5 different cultures of each cell line).

† Relative intensity of the EpRE-specific band in *14CoS/14CoS* cells is significantly higher ($P < 0.001$) than that in *ch/ch* cells.

Interestingly, the Fig. 2 data also demonstrate that *14CoS/14CoS*, although having the 3800-kb deletion on Chr 7 and exhibiting a constitutive oxidative stress response, are capable of even higher levels of oxidative stress response when challenged by tBHQ. This finding is inconsistent with the hypothesis [7] of a repressor gene (*Nmo1n*) proposed to be located in the Chr 7 deleted region.

Competition of EpRE-binding protein(s) by the AP-1 or AhRE DNA motif

The rat and human homologous *NMO1* genes, and the rat and mouse homologous *GSTA1* genes contain an AP-1-like EpRE in their 5′-flanking regulatory regions [32–34, 52]. We have cloned and sequenced the murine *Nmo1* [22], *Ahd4* (ALDH3c) [53], and *Ugt1*06* [38] genes, and found one or two EpRE motifs in the 5′-flanking regulatory regions of all three genes. We have previously reported [54] that the oxidative stress response in the *14CoS/14CoS* mouse—leading to elevated NMO1, ALDH3c, and UGT1*06 mRNA levels—is associated with the EpRE recognition sequences.

Is there any interaction between proteins binding to the EpRE and to the AhRE? Fig. 3 shows that both TCDD and tBHQ treatment (4th and 7th lanes) caused increases in the EpRE-binding protein band, compared with that of untreated cells (1st lane). An excess of unlabeled AP-1 was able to compete with the EpRE, causing the EpRE-specific band to disappear (2nd, 5th, and 8th lanes); these data are consistent with the data of Li and Jaiswal [33] who studied the human *NMO1* gene. Interestingly, an excess of unlabeled AhRE3 was also able to compete with the EpRE (though to a lesser degree than did AP-1), causing decreases in the EpRE-specific band (3rd, 6th, and 9th lanes). These experiments with Hepa-1 *wt* cells (Fig. 3) were repeated with the *ch/ch* cells and standardized with the control probe, Oct-1 (Fig. 4, Table 3). The results suggest that proteins binding to the AhRE are competing with proteins binding to the EpRE transcriptional complex.

This possibility was further supported by results from experiments with mutant DNA motifs. Figure 5 shows that unlabeled EpRE and AP-1 oligonucleotides were able to compete completely for the EpRE-specific band (lanes 2, 4, 9, & 11), whereas the other oligonucleotides

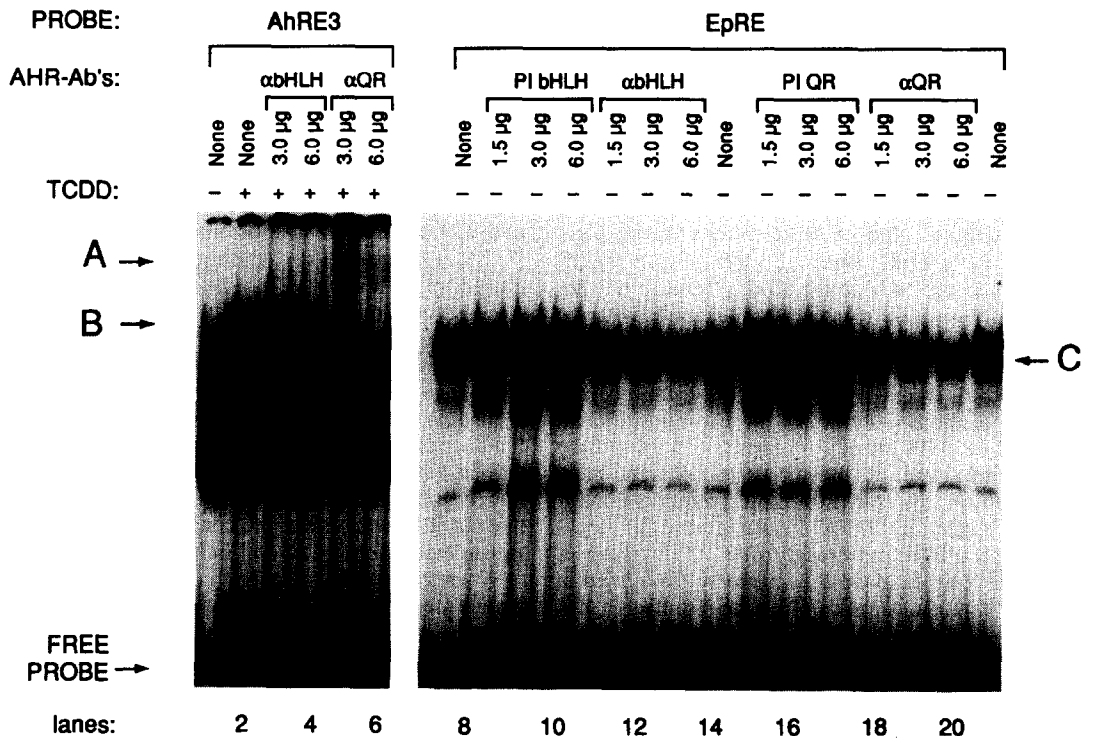

Fig. 6. Gel mobility shift analysis of Hepa-1 *wt* nuclear extracts probed with the radiolabeled *Gsta1* EpRE, and the effect of antibodies to the AHR. Cells were treated with 10 nM TCDD or vehicle alone for 6 hr. PI represents preimmune serum; α represents antibody. Band *B* denotes the AhRE-specific TCDD-inducible band. Band *A* denotes the antibody-supershifted AhRE-specific band. Band *C* denotes the EpRE-specific band.

decreased EpRE binding to a lesser degree, in the order of EpRE > mEpRE > AhRE3 > mAhRE3 > C/EBPα (standardized to the negative control, Oct-1). The mutated EpRE oligonucleotide, thus, competes less effectively than the wild-type EpRE sequence, and the mutated AhRE oligonucleotide competes less effectively than the wild-type AhRE sequence. These data suggest further that proteins binding to the AhRE are competing with proteins that bind to the EpRE DNA motif. The same competition was also found with C/EBPα (Fig. 5).

It should be pointed out that, within the mEpRE, there is a 9-bp sequence that contains the EpRE core binding site (TGACNNNGC; as in Table 1). Hence, we conclude that either both TGACNNNGC cores in the upstream region of the *Gsta1* gene are necessary for the EpRE-specific band or both sites are able to bind the same, or different, protein complexes. This can be resolved by using shorter oligonucleotide probes, as well as the longer probe having mutations in both core binding sites; these additional experiments are underway.

Differences in EpRE-binding protein(s) between the ch/ch *and* 14CoS/14CoS *cells*

Figure 5 shows that there is a qualitative increase in the EpRE band in nuclear extracts from untreated *14CoS/14CoS* (lane 1), as compared with that in untreated *ch/ch* (lane 8) cells. We, again, quantitated the difference by studying an Oct-1-specific band in the same extracts, determining that untreated *14CoS/14CoS* cells have more than twice as much EpRE-specific protein than untreated *ch/ch* cells (Table 4). These data show that there is a correlation between the increased oxidative stress response found in *14CoS/14CoS* cells and the increase in EpRE-binding protein(s). Interestingly, these results with untreated cells suggest that oxidative stress, to some degree, is occurring all the time as the result of endogenous metabolism.

Possible involvement of the Ah receptor in the EpRE-binding complex

The fact that the AhRE3 is able to compete partially with the EpRE-specific band (Figs. 3–5) suggested to us that the AHR, or other AhRE-binding protein, might participate in the EpRE-binding complex. Figure 6 (*left*) shows that an antibody to the AHR glutamine-rich region (αQR) was more effective than an antibody to the AHR bHLH region (αbHLH) in supershifting the AhRE3-specific band. The antibody supershifts increase as a function of increasing antibody. These data confirm that these antibodies, developed against two different portions of the AHR protein, are capable of supershifting and eliminating the gel mobility electrophoretic band that represents the AhRE-binding protein complex. More specifically, the TCDD-inducible band (*B*), negligible in lane 1, increases strongly after TCDD treatment of the cells (lane 2). Band *B* is markedly diminished in lanes 5 & 6 with appearance of the supershifted band *A* following incubation with the antibody αQR, whereas incubation with the antibody αbHLH had little effect (lanes 3 & 4).

Table 5 and Fig. 6 (*right*) show that both AHR antibodies are capable of blocking the interaction of EpRE-binding proteins with the EpRE motif, whereas incubation of preimmune serum with these nuclear extracts does not diminish formation of the EpRE-specific band *C*. We also found that an antibody to ARNT [55] did not cause a supershift of the EpRE band, although anti-ARNT was effective in causing a supershift of the AhRE band (Table 5). Furthermore, the AHR antibody-induced decreases in the EpRE band were proportional to the amount of antibody added. Qualitative changes seen in Fig. 6 were quantitated in three individual experiments; these results (Table 5) strongly suggest that the AHR, or a related protein, participates in the EpRE-binding complex.

Table 5. Densitometric analysis: Effect of the AHR antibodies on the EpRE-specific band, using nuclear extracts from Hepa-1 wt cells

Antibody (α) or Preimmune serum (PI)		% EpRE-specific band
None		100%
PI-1	1.5 μg	120
PI-1	3.0 μg	120
PI-1	6.0 μg	105
α-ARNT	3.0 μg	110
α-bHLH	1.5 μg	66
α-bHLH	3.0 μg	50
α-bHLH	6.0 μg	31
PI-2	1.5 μg	118
PI-2	3.0 μg	106
PI-2	6.0 μg	103
α-QR	1.5 μg	57
α-QR	3.0 μg	42
α-QR	6.0 μg	36

Values expressed are the average of 3 independent experiments, again, standardized by the negative control, Oct-1, as described in Tables 3 and 4.

CONCLUSIONS

In summary, in the deleted region of Chr 7 of *14CoS/14CoS* mice, this laboratory had postulated the presence of a "master switch" repressor gene—*Nmo1n*, a negative effector of *Nmo1* and the other [*Ah*] Phase II genes [7, 24]. The generation of endogenous oxidative stress, caused by the absence of a gene in this deleted region, was also considered a possibility [25]. From studies of transgenic and knockout *Fah* mouse lines [30, 31], it now appears likely that the latter hypothesis is the correct one and that the putative *Nmo1n* [7, 24], *hsdr1* [2, 5], and *alf* [8, 17] genes are one and the same. Using an inhibitor of an enzyme in the tyrosine degradation pathway in *Fah*(-/-) knockout mice, however, the expected downregulation of *Nmo1* was not found [56], indicating that not all answers are in yet, concerning the attempts to equate the *14CoS/14CoS* and *Fah*(-/-) mouse lines.

Whereas at least six genes in the [*Ah*] battery are upregulated by dioxin, the four [*Ah*] Phase II genes—but not the two [*Ah*] Phase I genes—are upregulated in response to endogenous or exogenous oxidative stress. From the work presented here, we suggest that oxidative stress occurs (*via* endogenous metabolism) in untreated cells, and the oxidative stress response can be increased by either endogenous or exogenous metabolites. The data shown in the present study also suggest the likelihood that the AHR participates in both the TCDD-inducible AhRE-mediated response and the oxidative

stress-inducible EpRE-mediated response. To our knowledge, this might be the first report in which the same transcription factor participates in two distinct transcriptional complexes, at two different response elements, upstream of a single gene. This is also the first incidence in which AHR might participate in a transcriptional complex in the absence of ARNT. A recent report has shown the converse: that ARNT, but not AHR, binds to the erythropoietin gene enhancer in response to hypoxia [57].

Furthermore, our findings show that, although further definitive experiments are needed, C/EBPα also appears to participate in the oxidative stress-inducible EpRE-mediated response. The possible competition of the same transcriptional factor (AHR), involved in two very different enhancers/DNA motifs upstream of the same gene (*Nmo1, Ahd4, Ugt1*06,* and *Gsta1*), upregulated by distinctly different signals, is intriguing and suggests many further experiments to explore this interrelationship. Is the role of the AHR in oxidative stress absolutely essential, or is it a redundant pathway? What is(are) the endogenous ligand(s) for the AHR? What other, and how many, proteins bind to the EpRE and to the AhRE? How does hypoxia-induced ARNT-mediated gene expression affect AHR-mediated gene expression? These questions are being pursued in our laboratories.

Acknowledgements—This work was supported by NIH Grants R01 AG09235 (D.W.N.), R01 ES06273 (A.P.), P30 ES06096 (A.P., M.W.T., D.W.N.), and P42 ES04908 (M.W.T.). We thank our colleagues for valuable discussions and a critical reading of this manuscript. V. Vasiliou was a Fogarty Scholar at the University of Cincinnati (1991–93). Most of these data were presented at the 32nd Annual Meeting of the Society of Toxicology, New Orleans, LA, in March, 1993 [54] and at "Molecular Toxicology" Conference, Keystone Symposia on Molecular and Cellular Biology, Copper Mountain, CO, in January, 1995 [58].

REFERENCES

1. Erickson RP, Gluecksohn-Waelsch S and Cori CF, Glucose-6-phosphatase deficiency caused by radiation-induced alleles at the albino locus in the mouse. *Proc Natl Acad Sci USA* **59:** 437–444, 1968.
2. Gluecksohn-Waelsch S, Genetic control of morphogenetic and biochemical differentiation: Lethal albino deletions in the mouse. *Cell* **16:** 225–237, 1979.
3. Russell LB, Montgomery CS and Raymer GD, Analysis of the albino-locus region of the mouse: Characterization of 34 deficiencies. *Genetics* **100:** 427–453, 1982.
4. Gluecksohn-Waelsch S, Regulatory genes in development. *Trends Genet* **3:** 123–127, 1987.
5. McKnight SL, Lane MD and Gluecksohn-Waelsch S, Is CCAAT/enhancer-binding protein a central regulator of energy metabolism? *Genes Dev* **3:** 2021–2024, 1989.
6. Rinchik EM, Tönjes RR, Paul D and Potter MD, Molecular analysis of radiation-induced *albino (c)*-locus mutations that cause death at preimplantation stages of development. *Genetics* **135:** 1107–1116, 1993.
7. Nebert DW, Petersen DD and Fornace AJ Jr, Cellular responses to oxidative stress: The [*Ah*] gene battery as a paradigm. *Environ Health Perspect* **88:** 13–25, 1990.
8. Ruppert S, Boshart M, Bosch FX, Schmid W, Fournier REK and Schütz G, Two genetically defined *trans*-acting loci coordinately regulate overlapping sets of liver-specific genes. *Cell* **61:** 895–904, 1990.
9. Thorndike J, Trigg MJ, Stockert R, Gluecksohn-Waelsch S and Cori CF, Multiple biochemical effects of a series of x-ray induced mutations at the albino locus in the mouse. *Biochem Genet* **9:** 25–39, 1973.
10. Schmid W, Müller G, Shütz G and Gluecksohn-Waelsch S, Deletions near the albino locus on chromosome 7 of the mouse affect the level of tyrosine aminotransferase mRNA. *Proc Natl Acad Sci USA* **82:** 2866–2869, 1985.
11. Loose DS, Shaw PA, Krauter KS, Robinson C, Englard S, Hanson RW and Gluecksohn-Waelsch S, *Trans* regulation of the phospho*enol*pyruvate carboxykinase (GTP) gene, identified by deletions in chromosome 7 of the mouse. *Proc Natl Acad Sci USA* **83:** 5184–5188, 1986.
12. Gonzalez FJ, Liu S-Y, Kozak CA and Nebert DW, Decreased *Hnf-1* gene expression in mice homozygous for a 1.2-centiMorgan deletion on chromosome 7. *DNA Cell Biol* **9:** 771–776, 1990.
13. DeFranco D, Morris Jr SM, Leonard CM and Gluecksohn-Waelsch S, Metallothionein mRNA expression in mice homozygous for chromosomal deletions around the albino locus. *Proc Natl Acad Sci USA* **85:** 1161–1164, 1988.
14. Morris Jr SM, Moncman CL, Kepka DM, Nebes, VL, Diven WF, Dizikes GJ, Cederbaum SD and DeFranco D, Effects of deletions in mouse chromosome 7 on expression of genes encoding the urea-cycle enzymes and phospho*enol*pyruvate carboxykinase (GTP) in liver, kidney, and intestine. *Biochem Genet* **26:** 769–781, 1988.
15. Tönjes RR, Xanthopoulos KG, Darnell Jr JE and Paul D, Transcriptional control in hepatocytes of normal and c^{14CoS} albino deletion mice. *EMBO J* **11:** 127–133, 1992.
16. Landegren U, Kaiser R, Caskey CT and Hood L, DNA diagnostics—Molecular techniques and automation. *Science* **242:** 229–237, 1988.
17. Kelsey G, Schedl A, Ruppert S, Niswander L, Magnuson T, Klebig ML, Rinchik EM, Schütz G, Physical mapping of the albino-deletion complex in the mouse to localize the *alf/hsdr-1*, a locus required for neonatal survival. *Genomics* **14:** 275–287, 1992.
18. Fornace AJ Jr, Nebert DW, Hollander MC, Luethy JD, Papathanasiou M, Fargnoli J and Holbrook NJ, Mammalian genes coordinately regulated by growth arrest signals and DNA-damaging agents. *Mol Cell Biol* **9:** 4196–4203, 1989.
19. Petersen DD, Gonzalez FJ, Rapic V, Kozak CA, Lee J-Y, Jones JE and Nebert DW, Marked increases in hepatic NAD(P)H:menadione oxidoreductase gene transcription and mRNA levels correlated with a mouse chromosome 7 deletion. *Proc Natl Acad Sci USA* **86:** 6699–6703, 1989.
20. Vasiliou V, Puga A and Nebert DW, Negative regulation of the murine cytosolic aldehyde dehydrogenase-3 (*Aldh-3c*) gene by functional CYP1A1 and CYP1A2 proteins. *Biochem Biophys Res Commun* **187:** 413–419, 1992.
21. Vasiliou V, Reuter SF, Kozak CA and Nebert DW, Mouse dioxin-inducible cytosolic aldehyde dehydrogenase-3: AHD4 cDNA sequence, genetic mapping, and differences in mRNA levels. *Pharmacogenetics* **3:** 281–290, 1993.
22. Vasiliou V, Theurer MJ, Puga A, Reuter SF, Nebert DW, Mouse dioxin-inducible NAD(P)H:menadione oxidoreductase: NMO1 cDNA sequence and genetic differences in mRNA levels. *Pharmacogenetics* **4:** 341–348, 1994.
23. Nebert DW and Gonzalez FJ, P450 genes: Structure, evolution and regulation. *Annu Rev Biochem* **56:** 945–993, 1987.
24. Nebert DW, Drug-metabolizing enzymes in ligand-modulated transcription. *Biochem Pharmacol* **47:** 25–37, 1994.
25. Liang HC, Shertzer HG and Nebert DW, "Oxidative stress" response in liver of an untreated newborn mouse having a 1.2-centiMorgan deletion on chromosome 7. *Biochem Biophys Res Commun* **182:** 1160–1165, 1992.
26. Yu M, Nebert DW and Jamieson GA Jr, Activation of dioxin-inducible genes in an untreated mouse cell line having a 1.2-cM deletion on chromosome 7: Evidence for arachidonic acid pathway involvement. *The Toxicologist* **12:** 195, 1992.
27. Liu R-M, Nebert DW and Shertzer HG, Menadione toxicity in two mouse liver established cell lines having striking

genetic differences in quinone reductase activity and glutathione concentrations. *Toxicol Appl Pharmacol* **122:** 101–107, 1993.

28. Klebig ML, Russell LB and Rinchik EM, Murine fumarylacetoacetate hydrolase (*Fah*) gene is disrupted by a neonatally lethal albino deletion that defines the hepatocyte-specific developmental regulation 1 (*hsdr-1*) locus. *Proc Natl Acad Sci USA* **89:** 1363–1367, 1992.
29. Ruppert S, Kelsey G, Schedl A, Schmid E, Thies E and Schütz G, Deficiency of an enzyme of tyrosine metabolism underlies altered gene expression in newborn liver of lethal albino mice. *Genes Dev* **6:** 1430–1443, 1992.
30. Kelsey G, Ruppert S, Beermann F, Grund C, Tanguay RM, Schütz G, Rescue of mice homozygous for lethal albino deletions: Implications for an animal model for the human liver disease tyrosinemia type I. *Genes Dev* **7:** 2285–2297, 1993.
31. Grompe M, Al-Dhalimy M, Finegold M, Ou C-N, Burlingame T, Kennaway NG, Soriano P, Loss of fumarylacetoacetate hydrolase is responsible for the neonatal hepatic dysfunction phenotype of lethal albino mice. *Genes Dev* **7:** 2298–2307, 1993.
32. Friling RS, Bergelson S and Daniel V, Two adjacent AP-1-like binding sites form the electrophile-responsive element of the murine glutathione S-transferase Ya subunit gene. *Proc Natl Acad Sci USA* **89:** 668–672, 1992.
33. Li Y and Jaisal AK, Regulation of human NAD(P)H:quinone oxidoreductase gene. Role of AP-1 binding site contained within human antioxidant response element. *J Biol Chem* **267:** 15097–15104, 1992.
34. Rushmore TH, Morton MR and Pickett CB, The antioxidant responsive element. Activation by oxidative stress and identification of the DNA consensus sequence required for functional activity. *J Biol Chem* **266:** 11632–11639, 1991.
35. Bernard HP, Darlington GJ and Ruddle FH, Expression of liver phenotypes in cultured mouse hepatoma cells: Synthesis and secretion of serum albumin. *Dev Biol* **35:** 83–96, 1974.
36. Benedict WF, Gielen JE, Owens IS, Niwa A and Nebert DW, Aryl hydrocarbon hydroxylase induction in mammalian liver cell culture. IV. Stimulation of the enzyme activity in established cell lines derived from rat or mouse hepatoma and from normal rat liver. *Biochem Pharmacol* **22:** 2766–2769, 1973.
37. Kimura S, Smith HH, Hankinson O and Nebert DW, Analysis of two benzo[a]pyrene-resistant mutants of the mouse hepatoma Hepa-1 P_1450 gene via cDNA expression in yeast. *EMBO J* **6:** 1929–1933, 1987.
38. Chomczynski P and Sacchi N, Single-step method of RNA isolation by acid guanidinium thiocyanate-phenol-chloroform extraction. *Anal Biochem* **162:** 156–159, 1987.
39. Reuter SF, Vasiliou V, Puga A and Nebert DW, Characterization of the murine dioxin-inducible UDP glucuronosyltransferase (*Ugt1*06*) gene. *The Toxicologist* **14:** 410, 1994.
40. Tabor MW, Protocol for the separation of residue organics for mutagenicity testing. In: *Guidelines for Preparing Environmental and Waste Samples for Mutagenicity (Ames) Testing: Interim Procedures.* (Ed. Williams LR) Technical Monitor, USEPA Office of Research and Development, Washington, DC, USEPA/600/4-85/058, pp. 227–240, 1985.
41. Bory C, Boulieu R, Chantin C and Mothieu M, Diagnosis of alcaptonuria: Rapid analysis of homogentisic acid by HPLC. *Clin Chim Acta* **189:** 7–12, 1990.
42. Tabor MW, Chromatography: principles and theory. In: *Clinical Chemistry—Theory, Analysis and Correlation,* 3rd ed. (Ed. Pesce AJ), pp. 106–127. C.V. Mosby, Inc., St. Louis, 1995.
43. Puga A, Raychaudhuri B and Nebert DW, Transcriptional depression of the murine *Cyp1a1* gene by mevinolin. *FASEB J* **6:** 777–785, 1992.
44. Carrier F, Chang CY, Duh JL, Nebert DW and Puga A, Interaction of the regulatory domains of the murine *Cyp1a1* gene with two DNA-binding proteins in addition to the Ah receptor and the Ah receptor nuclear translocator (ARNT). *Biochem Pharmacol* **48:** 1767–1778 1994.
45. Cao Z, Umek RM, and McKnight SL, Regulated expression of three C/EBP isoforms during adipose conversion of 3T3-L1 cells. *Genes Dev* **5:** 1538–1552, 1991.
46. Burbach KM, Poland AP and Bradfield CA, Cloning of the Ah receptor cDNA reveals a distinctive ligand-activated transcription factor. *Proc Natl Acad Sci USA* **89:** 8185–8189, 1992.
47. Lindblad B, Lindstedt S and Steen G, On the enzymic defects in hereditary tyrosinemia. *Proc Natl Acad Sci USA* **74:** 4641–4645, 1977.
48. Tuchman M, Freese DK, Sharp HL, Whitley CB, Ramnaraine ML, Ulstrom RA, Najarian JS, Ascher N, Buist NR and Terry AB, Persistent succinylacetone excretion after liver transplantation in a patient with hereditary tyrosinemia type I. *J Inherit Metab Dis* **8:** 21–24, 1985.
49. Collins JC, Buchanan DN, Thoene JG, Erickson RP, Brooks SS and Gluecksohn-Waelsch S, Metabolic studies in a mouse model of hepatorenal tyrosinemia: Absence of perinatal abnormalities. *Biochem Biophys Res Commun* **187:** 340–346, 1992.
50. Stoner E, Starkman H, Wellner D, Wellner VP, Sassa S, Rifkind AB, Grenier A, Steinherz PG, Meister A, New MI and Levine LS, Biochemical studies of a patient with hereditary hepatorenal tyrosinemia: Evidence of glutathione deficiency. *Pediat Res* **18:** 1332–1336, 1984.
51. Vasiliou V, Puga A and Nebert DW, Mouse class 3 aldehyde dehydrogenases: Positive and negative regulation of gene expression. *Adv Exp Med Biol* **328:** 131–139, 1993.
52. Jaiswal AK, Human NAD(P)H:quinone oxidoreductase (NQO_1) gene structure and induction by dioxin. *Biochemistry* **30:** 10647–10653, 1991.
53. Vasiliou V, Reuter SF and Nebert DW, Organization and characterization of the murine dioxin-inducible cytosolic aldehyde dehydrogenase (*Ahd4*) gene. *The Toxicologist* **14:** 410, 1994.
54. Nebert DW, Puga A, Tabor MW and Vasiliou V, Involvement of the electrophile-responsive element (EpRE) in the murine chromosome 7-mediated depression of the Phase II [*Ah*] battery genes. *The Toxicologist* **13:** 135, 1993.
55. Hord NG and Perdew GH, Physiological and immunocytochemical analysis of the aryl hydrocarbon receptor nuclear translocator: Characterization of two monoclonal antibodies to the aryl hydrocarbon receptor translocator. *Mol Pharmacol* **46:** 618–626, 1994.
56. Grompe M, Lindstedt S, Al-Dhalimy M, Kennaway NG, Papaconstantinou J, Torres-Ramos CA, Ou CN and Finegold M, Pharmacological correction of neonatal lethal hepatic dysfunction in a murine model of hereditary tyrosinemia type I. *Nature Genet* **10:** 453–460, 1995.
57. Wang GL, Jiang BH, Rue EA and Semenza GL, Hypoxia-inducible factor 1 is a basic-helix-loop-helix-PAS heterodimer regulated by cellular O_2 tension. *Proc Natl Acad Sci USA* **92:** 5510–5514, 1995.
58. Nebert DW, Liang HC, Reuter SF, McKinnon RA, Shertzer HG, Puga A and Vasiliou V, Role of the murine [*Ah*] gene battery in oxidative stress. *J Cell Biochem Suppl.* **19A:** 183, 1995.